

# Distributionally robust multi-period energy management for CCHP-based microgrids

ISSN 1751-8687  
 Received on 12th March 2020  
 Revised 11th June 2020  
 Accepted on 12th June 2020  
 E-First on 10th July 2020  
 doi: 10.1049/iet-gtd.2020.0469  
 www.ietdl.org

Zhichao Shi<sup>1</sup> ✉, Hao Liang<sup>1</sup>, Venkata Dinavahi<sup>1</sup>

<sup>1</sup>Department of Electrical and Computer Engineering, University of Alberta, Edmonton, AB, Canada

✉ E-mail: zhichao1@ualberta.ca

**Abstract:** To improve the overall energy utilisation efficiency, the research of combined cooling, heat, and power (CCHP)-based microgrids has become prevalent recently. However, the increasing penetration of uncertain renewable generation such as wind power brings new challenges to CCHP-based microgrids energy management. In this study, the authors propose a two-stage multi-period distributionally robust energy management model for CCHP-based microgrids, and this model considers the non-anticipativity of uncertainty in dispatch process. A second-order conic representable ambiguity set is designed to capture the uncertainty of wind power. Based on linear decision rule approximation, the proposed problem is transformed into a tractable mixed-integer second-order conic programme problem. Case studies and comparison experiments are conducted in the Matlab environment with real-world data to validate the performance of the proposed approach. Particularly, the proposed method achieves a less conservative solution and smaller cost compared with a robust optimisation method with the same reliability guarantee. In addition, it is more reliable than the deterministic method which does not consider uncertainty.

## Nomenclature

### Parameters

$i/g/j/m/n$	indices of microturbine (MT)/gas furnace/electric energy storage system (ESS)/ thermal storage system (TSS)/wind farm
$c^{\text{air}}$	air specific heat capacity, kWh/°C
$c^{\text{gas}}$	price of natural gas, \$/m <sup>3</sup>
$c_i^{\text{NL}}$	no load cost coefficient of MT $i$
$c_j^e/c_m^q$	degradation cost coefficient of ESS/TSS, \$/kWh
$c_i^{\text{buy}}/c_i^{\text{sell}}$	electricity exchange price, \$/kWh
$\text{COP}^{\text{C}}/\text{COP}^{\text{H}}$	cooling/heating coefficient of performance
$\text{DT}_i/\text{UT}_i$	minimum down-time/up-time of unit $i$
$E_{j0}^e/E_{m0}^q$	initial storage level of ESS/TSS, kWh
$\underline{E}_j^e/\bar{E}_j^e$	minimum/maximum storage level of ESS, kWh
$\underline{E}_m^q/\bar{E}_m^q$	minimum/maximum storage level of TSS, kWh
$\underline{h}_g^{\text{GF}}/\bar{h}_g^{\text{GF}}$	minimum/maximum output of gas furnace $g$ , kW
$H^{\text{G}}$	heat value of natural gas, kWh/m <sup>3</sup>
$\bar{p}^{\text{AC}}/\bar{p}^{\text{HC}}$	maximum supplied cooling/heating power, kW
$\underline{p}_i/\bar{p}_i$	minimum/maximum output of unit $i$ , kW
$p_i^{\text{load}}$	load demand at time $t$ , kW
$\underline{r}_j^e/\bar{r}_j^e$	lower/upper limit of charging of ESS $j$ , kW
$\underline{r}_j^e/\bar{r}_j^e$	lower/upper limit of discharging of ESS $j$ , kW
$\underline{r}_m^q/\bar{r}_m^q$	lower/upper limit of charging of TSS $m$ , kW
$\underline{r}_m^q/\bar{r}_m^q$	lower/upper limit of discharging of TSS $m$ , kW
$R_i^{\text{dn}}/R_i^{\text{up}}$	ramp-down/ramp-up limit of unit $i$ , kW
$R^{\text{tr}}$	thermal resistance of building, °C/kW
$\eta_i^{\text{MT}}$	efficiency coefficient of MTs
$\eta_i^{\text{MT,loss}}$	loss coefficient of MTs
$\eta_g^{\text{GF}}$	output efficiency of gas furnace
$\theta_t^{\text{am}}$	ambient temperature at time $t$ , °C
$\underline{\theta}_t^{\text{in}}/\bar{\theta}_t^{\text{in}}$	lower/upper limit of indoor temperature at time $t$ , °C
<b>Variables</b>	
$F_{it}$	natural gas consumption of unit $i$ at time $t$ , m <sup>3</sup>

$h_{it}^{\text{MT}}$	heat output of MTs, kW
$h_{gt}^{\text{GF}}$	heat output of gas furnace, kW
$p_{it}$	electric output of MTs, kW
$p_i^{\text{AC}}/p_i^{\text{HC}}$	supplied cooling/heating power, kW
$p_i^{\text{buy}}/p_i^{\text{sell}}$	electricity purchased from/sold to the main grid, kW
$q_t^{\text{CE}}/q_t^{\text{HE}}$	energy conveyed to cooling/heat load, kWh
$r_{jt}^{e+}/r_{jt}^{e-}$	charging/discharging of ESS, kW
$r_{mt}^{q+}/r_{mt}^{q-}$	charging/discharging of TSS, kW
$u_{nt}/v_{kt}$	auxiliary variables in the lifted ambiguity set
$w_{nt}$	wind power of wind farm $n$ at time $t$ , kW
$\mathbf{x}$	second-stage decision vector
$y_{it}/y_{it}^+/y_{it}^-$	binary variables indicating on-off status/start-up/shut-down
$\mathbf{y}$	first-stage decision vector
$\theta_t^{\text{in}}$	indoor temperature settings, °C

## 1 Introduction

Compared with conventional fossil fuels, renewable energies such as wind and solar energy are clean and pollution-free, and they have been increasingly utilised in power system operation in recent years. Renewable generation integration is a popular trend in the future smart grid, and this also facilitates the development and research of microgrids in the past few decades. Among various microgrids, one interesting kind is the combined cooling, heating, and power (CCHP)-based microgrid, which is also known as the tri-generation system, and it can provide electric and thermal power simultaneously [1, 2]. A CCHP-based microgrid usually consists of renewable generation, CCHP units such as microturbines (MTs), heating and refrigeration systems, and different kinds of loads. The energy utilisation efficiency can be significantly improved (e.g. to be 80%) by implementing CCHP in a microgrid compared with traditional independent energy systems [3]. Therefore, the CCHP microgrid is considered a leading power generation method in the electricity market with efficiency and environmental concern.

There are generally two operational modes for CCHP units in practice, i.e. following the electric load and following the thermal load depending on the priority of load satisfaction [4]. To decouple

the electric and thermal output of CCHP units, storage systems are usually utilised in the microgrid operation. Energy management or dispatch for CCHP-based microgrids has been widely studied with various strategies and methods. For example, in [5], a coordinated operation strategy is proposed for a distribution system integrated with gas–electricity and CCHP units, and the accurate forecast of renewable generation is used. Similarly, an optimal dispatch strategy for a CCHP system is proposed to minimise the total operation cost with forecasted wind power in [6]. In addition, an interconnected two-area hybrid microgrid system with wind energy is studied in [7] and robust model predictive control (MPC) is designed for load frequency and voltage control. In [8], bio-renewable cogeneration-based hybrid microgrids are studied for energy management with demand response, and the microgrids include both renewable generation units and CHP units. Renewable energy data in these works are also forecasted values or certain average values. However, forecast errors for renewable generation cannot be eliminated fully and exact forecast values can hardly be obtained in practice.

The increasing penetration of renewable generation has brought new challenges to microgrid energy management, which also makes uncertainty modelling a necessity. In addition, variable load and electricity price can also introduce uncertainties in the electricity market. To cope with these uncertainties, two typical methods including stochastic programming and robust optimisation have been investigated for microgrid energy management. In stochastic programming methods, a certain probability distribution is usually used for random variables or its forecast error. For example, the optimal short-term scheduling of combined heat and power (CHP)-based microgrids is studied in [9], where a stochastic programming formulation is adopted with a Weibull distribution assumption of wind speed. The coordinated day-ahead scheduling and real-time dispatch models are developed for the coupled co-optimisation of cooling and electric energy in [10], and the uncertainty of wind power is represented by multiple scenarios generated from a normal distribution. Similarly, the temporally-coordinated optimal operation for a CCHP-based microgrid is investigated in [11], and this work considers multiple uncertainties from renewable generation, load demand, and electricity transaction price with a stochastic programming model. In [12], a stochastic-robust coordination optimisation model is proposed for CCHP-based microgrids, which uses stochastic scenarios and uncertainty set to represent the uncertain electricity prices and renewable generation, respectively. The limitation of the stochastic programming method is that it usually suffers from a high computational burden with many scenarios. In addition, the true probability distribution cannot be known exactly in practice.

Compared with the stochastic optimization method, robust optimisation does not need the true distribution assumption, and it has also been a popular method to handle the uncertainties. In [13], a two-stage new robust coordinated operation method is proposed for a grid-connected CCHP-based microgrid, and multiple uncertainties are considered based on uncertainty sets. Similarly, a two-stage adaptive robust optimisation approach is developed in [14] for energy management of a microgrid with CHP units and uncertain wind power. In [15], a robust model based on information gap decision theory is formulated to derive the optimal operation strategy for CHP units, and the envelope bound model is used for uncertainty modelling in this work. Although a robust optimisation method has fewer requirements on distribution information, it usually aims to find the optimal solution under the worst-case scenario of uncertainty which is often over-conservative or over-optimistic.

As an intermediate method, which can overcome the shortcomings of stochastic programming and robust optimisation methods, a new uncertainty modelling technique, distributionally robust optimisation (DRO), has been proposed and studied recently [16, 17]. In the DRO method, it is assumed that partial distribution information is known such as the first- and second-order moments, which makes it more practical than the stochastic method and less conservative than a robust method. It evaluates the worst-case expectation cost over all possible distributions described by a so-called ambiguity set. So far, this technique has been widely studied

in power system optimisation problems including the energy and reserve dispatch [18, 19], unit commitment (UC) [20], optimal power flow [21], and so on. In addition, a few works have also been reported for microgrid energy management with the DRO method. In [22], a distributionally robust chance-constrained energy management model for island microgrids is proposed with uncertain wind power, and the model is actually a single-stage model. With a moment-based ambiguity set, a day-ahead DRO model is developed in [23] and the problem is transformed into a two-stage mixed-integer linear programming problem.

Based on the above analysis, it can be found that distributionally robust energy management has seldom been studied for CCHP-based microgrids. The energy management of CCHP-based microgrids is usually more complex, which needs to consider the flow of electric energy and thermal energy simultaneously. Therefore, compared with traditional power systems, CCHP-based microgrids energy management with the DRO modelling method would be more complicated with the inclusion of more constraints. In addition, the existing works about CCHP-based microgrids mainly focus on the single-stage or two-stage models that ignore the non-anticipativity of dispatch decisions [24]. More specifically, in a general two-stage model, the uncertainty realisations for the whole horizon (e.g. 24 h) are all assumed to be known and the problem can be fully optimised in the second-stage dispatch process [25]. However, this assumption is unrealistic because we can only know uncertainty realisations up to current time in real-time dispatch processes and the future uncertainty information is unknown. Therefore, to enforce the non-anticipativity of dispatch decisions, a multi-period energy management model for CCHP-based microgrids with the DRO technique is proposed. Although non-anticipativity considerations have been studied in some problems such as robust UC [24], robust energy management [26], and stochastic hydropower scheduling [27], they are mostly studied in the robust model or stochastic optimisation model, and the combination with the DRO model for CCHP-based microgrids is not reported. As mentioned above, the DRO technique has advantages over stochastic programming and robust optimisation. Unlike the certain distribution assumption in stochastic programming, the DRO method assumes that only partial distribution information is known, and it is also less conservative than a robust optimisation method. In addition, considering the drawbacks in existing works such as the neglect of non-anticipativity of uncertainty, a multi-period model is studied, which is more realistic.

Specifically, in this work, the proposed multi-period model is included in a two-stage framework, and here the term multi-period instead of multi-stage is used to make a difference. To capture the uncertain distribution of renewable generation such as wind power, the DRO method is investigated and we design a new second-order conic representable ambiguity set. As the proposed distributionally robust multi-period energy management model is generally intractable, the linear decision rule (LDR) is further explored to help reformulate the problem as a tractable problem. The two-stage model and real-time optimisation have also been studied for microgrids with other methods such as model predictive control (MPC) [28–30]. However, the proposed approach is different from MPC and has some advantages compared with it. In the MPC method, many scenarios are usually required for the day-ahead stochastic optimisation, which is computationally heavy. In intraday operation, the forecast of uncertain wind power is updated gradually and the problem is solved in a rolling horizon [30]. By comparison, the distribution assumption of uncertain wind power and scenarios generation is not required in the proposed approach, which can help reduce the computational burden. In addition, the proposed method can solve the problem to obtain the first-stage decision and LDR for the second-stage variables, which can be used in the real-time operation when uncertain wind power is revealed. In other words, it is not necessary to run the simulation repeatedly in a rolling horizon as is done in the MPC method. In summary, the main contributions of this study are as follows:

- A novel two-stage multi-period distributionally robust model is proposed.

A two-stage multi-period energy management model is proposed for CCHP-based microgrids which consider the non-anticipativity of dispatch decisions, the proposed model is different from the common two-stage model, which ignores the non-anticipativity; and the DRO technique is adopted as the uncertainty modelling method.

- A new ambiguity set is designed.

A new second-order conic representable ambiguity set is designed to capture the uncertain distribution of wind power, and this moment-based set can describe the temporal and spatial correlation of random variable. Compared with previous moment-based ambiguity sets, partial cross-moment information is considered in this new ambiguity set. In addition, the linear decision rule is investigated to help transform the multi-period problem into a tractable problem.

- A new tight support set is developed.

Together with the lifted ambiguity set, a tight support set with upper bounds is developed to further improve the solutions, i.e. the conservativeness of the solutions is reduced by considering the new support set. Case studies are carried out based on real-world data, and the proposed approach is compared with other methods to verify its performance.

Compared with previous literature, there are several outstanding novelties in this work. First, a distributionally robust multi-period model for microgrids considering non-anticipativity is proposed, which has not been studied before. Second, a new ambiguity set is designed for the uncertainty modelling of renewable generation. In addition, different support sets in the ambiguity set are analysed.

The rest of this paper is organised as follows. The proposed CCHP-based microgrid system model and two-stage multi-period formulation are introduced in Section 2. In Section 3, we demonstrate the new ambiguity set and derive the solution methodology based on the linear decision rule. Case studies are conducted to show the results and performance of the proposed approach in Section 4. Finally, Section 5 concludes this study.

## 2 Problem formulation

In this section, the CCHP-based microgrid system structure and model framework are introduced first. Then the detailed models of the microgrid components including CCHP units, storage systems, electric and thermal load balance are formulated. Finally, the multi-period problem formulation is presented.

Microgrids can be operated in grid-connected or islanded mode. Since CCHP systems are usually connected to the utility grid in a distribution system, therefore, in this work, we will study the energy management of a grid-connected CCHP-based microgrid, which usually consists of conventional generation units such as MTs, renewable generation, storage systems, electric load, and thermal load. The basic structure and energy flows of a CCHP-based microgrid are depicted in Fig. 1, and this is also the proposed microgrid system model in this study. As shown in this figure, there are two energy flows: electric energy and thermal energy to satisfy the electric load and thermal load, respectively. Since the cooling load can be met by transforming some amount of heat energy with the absorption chiller, the heat and cooling loads are combined together here [13]. For the energy supply, MTs can generate electric energy and heat energy simultaneously, and the microgrid can exchange energy with the main grid. Considering the coupling nature of MTs, the gas furnace and thermal storage system are introduced to flexibly supply enough heat power.

In this work, a two-stage multi-period energy management model is studied for CCHP-based microgrids, specifically, we investigate the day-ahead scheduling of MTs in the first stage and study multi-period dispatch considering non-anticipativity in the second stage. The proposed model can be illustrated in Fig. 2. Note that in the second stage, the multi-period model with uncertain renewable generation is difficult to solve. Therefore, the LDR method is introduced to deal with non-anticipativity, which helps reformulate the original problem into a tractable problem. The objective is to minimise the total system cost including the first-stage scheduling cost of MTs and the second-stage dispatch cost

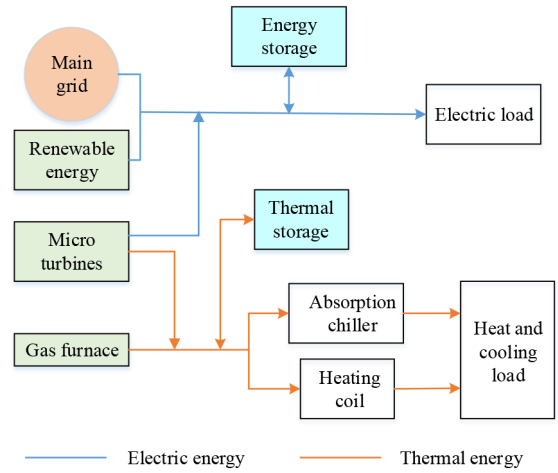


Fig. 1 Scheme of a grid-connected CCHP microgrid

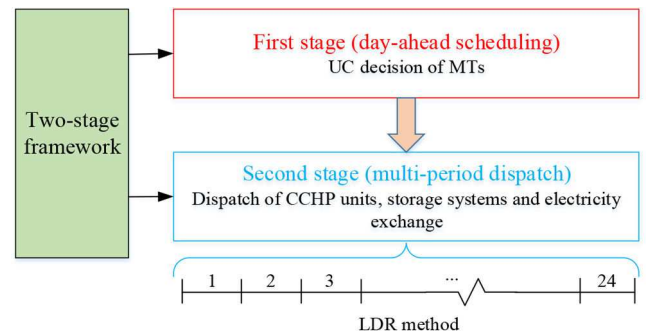


Fig. 2 Framework of the two-stage model

such as fuel cost and electricity exchange cost, and the detailed objective function will be introduced later.

### 2.1 CCHP units

In a CCHP-based microgrid, the most important component is the CCHP unit, which can significantly improve the overall energy utilisation efficiency by fully utilising the waste heat from generating electricity. For CCHP units in the studied system, MTs are used, which can directly generate power with natural gas. Specifically, the electric and heat output power of MTs are expressed as follows [3]:

$$p_{it} = F_{it} H^G \eta_i^{MT}, \quad \forall i, t \quad (1)$$

$$h_{it}^{MT} = F_{it} H^G (1 - \eta_{i,loss}^{MT} - \eta_i^{MT}) \quad (2)$$

where (1) represents the electric output of MTs and (2) represents the heat output,  $F_{it}$  is the natural gas consumption of unit  $i$  at time  $t$ ,  $H^G$  is the heat value of gas,  $\eta_i^{MT}$  is the efficiency coefficient and  $\eta_{i,loss}^{MT}$  is the loss coefficient of unit  $i$ . The mode of following the electric load is used in this work, and the complementarity of heat and power from MTs may be considered in the future by adding more related equipment.

As conventional generation units, the start-up/shut-down operation, minimum on time and off time limits should be considered in the day-ahead stage [14]. The related constraints are given below

$$-y_{i(t-1)} + y_{it} - y_{is} \leq 0, \quad \forall i, t, 1 \leq s - (t-1) \leq UT_i \quad (3)$$

$$y_{i(t-1)} - y_{it} + y_{is} \leq 1, \quad \forall i, t, 1 \leq s - (t-1) \leq DT_i \quad (4)$$

$$y_{it} - y_{i(t-1)} = y_{it}^+ - y_{it}^-, y_{it}^+ + y_{it}^- \leq 1, \quad \forall i, t \quad (5)$$

$$y_{it}, y_{it}^+, y_{it}^- \in \{0, 1\}, \quad \forall i, t \quad (6)$$

where constraints (3) and (4) represent the minimum on time and off time constraints, respectively, constraint (5) restricts the relationship between the status and the start-up/shut-down operation,  $y_{it}, y_{it}^+, y_{it}^-$  in (6) are binary variables representing the on/off status, start-up and shut-down operation of MTs, respectively.  $s$  is a time index, UT <sub>$i$</sub>  and DT <sub>$i$</sub>  represent the minimum up-time and down-time of unit  $i$ , respectively.

In addition, the generation capacity limit, ramping up/down restriction for MTs should also be considered, which are represented as below

$$y_{it} p_i \leq p_{it} \leq y_{it} \bar{p}_i, \quad \forall i, t \quad (7)$$

$$p_{it} - p_{i(t-1)} \leq \bar{p}_i y_{it}^+ + R_i^{\text{up}} y_{it}^-, \quad \forall i, t \quad (8)$$

$$p_{i(t-1)} - p_{it} \leq \bar{p}_i y_{it}^- + R_i^{\text{dn}} y_{it}^-, \quad \forall i, t \quad (9)$$

where constraint (7) denotes the output limit, constraints (8) and (9) ensure that the generation units do not ramp power output more than the predefined up and down ramp rates.

Considering the coupling electric and heat output of MTs, other heating devices such as gas furnace can be introduced to supply sufficient heat power in this system. A gas furnace generates heat power by combusting natural gas and the output constraints are as follows [3]:

$$h_{gt}^{\text{GF}} = F_{gt}^{\text{GF}} H^G \eta_g^{\text{GF}}, \quad \forall g, t \quad (10)$$

$$h_g^{\text{GF}} \leq h_{gt}^{\text{GF}} \leq \bar{h}_g^{\text{GF}}, \quad \forall g, t \quad (11)$$

where (10) describes the relationship between the output and gas consumption, constraint (11) represents the output limit,  $F_{gt}^{\text{GF}}$  is the gas consumption of unit  $g$  at time  $t$ , and  $\eta_g^{\text{GF}}$  is the output efficiency. Note that the heat power can be transformed into cooling power via absorption chillers to meet the cooling load, and the conversion model will be introduced later in Section 2.3.

## 2.2 Storage systems

Energy storage systems can play an important role in the energy supply of a microgrid. Both the electric energy storage system (ESS) and thermal storage system (TSS) can be used in a CCHP-based microgrid. For the ESS system, it should satisfy the charging and discharging restrictions at each time slot, and the storage level should be limited by the lower and upper bounds in the whole horizon, which can be expressed below [24]

$$\underline{r}_{jt}^e \leq r_{jt}^e \leq \bar{r}_{jt}^e, \underline{r}_{jt}^e \leq r_{jt}^e \leq \bar{r}_{jt}^e, \quad \forall j, t \quad (12)$$

$$\underline{E}_j \leq E_{j0}^e + \sum_{\tau \in [1:t]} (r_{j\tau}^e \eta_{j\tau}^e - r_{j\tau}^e / \eta_{j\tau}^e) \Delta t \leq \bar{E}_j, \quad \forall j, t \quad (13)$$

where  $r_{jt}^e$  and  $r_{jt}^e$  represent the charging and discharging of ESS  $j$  at time  $t$ , respectively.  $E_{j0}^e$  denotes the initial energy storage level,  $\eta_{j\tau}^e$  and  $\eta_{j\tau}^e$  are charging and discharging efficiency, respectively. Constraint (12) describes the charging and discharging limits, and constraint (13) restricts the storage level. Note that the binary variables to control the charging state of ESS are not considered here since the complementary constraint is redundant when the charging and discharging efficiency are included which has been demonstrated in related references [22, 31]. In addition, although it is common to set the final storage level to be the same with the beginning of the day for the sustainability of the storage system, it is not necessary since the optimisation problem can be solved with any initial storage level. The critical variables are the charging and discharging of the storage system in the proposed multi-period model, which also determines the storage level. Similarly, the energy storage dynamics and related constraints of TSS are represented as follows:

$$\underline{r}_m^q \leq r_{mt}^q \leq \bar{r}_m^q, \underline{r}_m^q \leq r_{mt}^q \leq \bar{r}_m^q, \quad \forall m, t \quad (14)$$

$$\underline{E}_m \leq E_{m0}^q + \sum_{\tau \in [1:t]} (r_{m\tau}^q \eta_{m\tau}^q - r_{m\tau}^q / \eta_{m\tau}^q) \Delta t \leq \bar{E}_m, \quad \forall m, t \quad (15)$$

where  $r_{mt}^q$  and  $r_{mt}^q$  are charging and discharging of TSS  $m$  at time  $t$ , and  $E_{m0}^q$  is the initial storage level of TSS  $m$ .

## 2.3 Load balance and objective

As discussed above, there are electric energy flow and thermal energy flow in the CCHP-based microgrid system, which are used to satisfy the corresponding loads. Based on the heat power from MTs, gas furnace, and TSS, the thermal load balance can be expressed as follows:

$$\sum_{i=1}^{N^{\text{MT}}} h_{it}^{\text{MT}} + \sum_{g=1}^{N^{\text{GF}}} h_{gt}^{\text{GF}} + \sum_{m=1}^{N^q} (r_{mt}^q - r_{mt}^q) = p_t^{\text{HC}} + p_t^{\text{AC}}, \quad \forall t \quad (16)$$

$$0 \leq p_t^{\text{HC}} \leq \bar{p}^{\text{HC}}, 0 \leq p_t^{\text{AC}} \leq \bar{p}^{\text{AC}}, \quad \forall t \quad (17)$$

where  $p_t^{\text{HC}}$  and  $p_t^{\text{AC}}$  are the heat power supplied to the heating coil and absorption chiller [13], respectively, as shown in Fig. 1. The final energy conveyed to the demand is limited by the device's coefficient of performance, and the conversion relation is given below

$$q_t^{\text{HE}} = p_t^{\text{HC}} \Delta t \cdot \text{COP}^{\text{H}}, q_t^{\text{CE}} = p_t^{\text{AC}} \Delta t \cdot \text{COP}^{\text{C}}, \quad \forall t. \quad (18)$$

The CCHP-based microgrid system is usually used in smart buildings such as residential houses or commercial buildings. In this work, the system is assumed to be balanced and only balanced loads are considered so that we only need to consider the simplified single-phase model, which is common in the previous literature. To make the proposed CCHP-based microgrid model more realistic, we consider the temperature-dependent thermal load in this work. In addition, the dynamics of the heating and cooling system such as the air conditioning system can be described by setting the indoor temperature. Specifically, the thermal load can be modelled by the thermodynamic equation, which is dependent on the indoor temperature setpoint and environmental temperature as follows [32]:

$$(q_t^{\text{HE}} - q_t^{\text{CE}}) / \Delta t = c^{\text{air}} (d\theta^{\text{in}} / dt) - (\theta_t^{\text{am}} - \theta_t^{\text{in}}) / R^{\text{tr}}, \quad \forall t \quad (19)$$

where  $c^{\text{air}}$  is a coefficient representing the air specific heat capacity,  $\theta^{\text{in}}$  and  $\theta^{\text{am}}$  are the indoor and ambient temperature, respectively, and  $R^{\text{tr}}$  is the thermal resistance of building envelop.

Considering the inertia of thermal energy, the indoor temperature actually alters slowly and it can be regarded as a constant within each time slot (e.g. 1 h). Therefore, the thermodynamic equation in (19) can be transformed into a discrete state model as below

$$(q_t^{\text{HE}} - q_t^{\text{CE}}) / \Delta t = c^{\text{air}} (\theta_t^{\text{in}} - \theta_{t-1}^{\text{in}}) / \Delta t - (\theta_t^{\text{am}} - \theta_t^{\text{in}}) / R^{\text{tr}}, \quad \forall t. \quad (20)$$

With this model, the thermal load can be controlled by setting different indoor temperatures. As the comfortable indoor temperature usually has a certain range, we also have the following constraint:

$$\underline{\theta}_t^{\text{in}} \leq \theta_t^{\text{in}} \leq \bar{\theta}_t^{\text{in}}, \quad \forall t. \quad (21)$$

where  $\underline{\theta}_t^{\text{in}}$  and  $\bar{\theta}_t^{\text{in}}$  are the predefined lower and upper bounds of indoor temperature. Note that the electric appliances and human activities in the building can also generate heat, e.g. the cooking activity and fitness exercises, while their impacts on the indoor

temperature and outdoor temperature are usually minor, which can be ignored.

Without loss of generality, wind power is considered as the renewable generation in this work. Combining the output power of MTs, ESS, and the electricity exchange with the main grid, the constraints about electric load balance are expressed as follows:

$$\sum_{i=1}^{N^{MT}} p_{it} + \sum_{j=1}^{N^e} (r_{jt}^- - r_{jt}^+) + \sum_{n=1}^{N^w} w_{nt} + p_t^{\text{buy}} - p_t^{\text{sell}} = p_t^{\text{load}}, \quad \forall t \quad (22)$$

$$0 \leq p_t^{\text{buy}} \leq \bar{p}^{\text{buy}}, 0 \leq p_t^{\text{sell}} \leq \bar{p}^{\text{sell}}, \quad \forall t \quad (23)$$

where  $w_{nt}$  represents the uncertain wind power, and its uncertainty modelling with the DRO method is introduced in the next section. For the main grid, we can purchase electricity from or sell excess power to it with the power flow limit.

The proposed energy management for CCHP-based microgrids is formulated in a two-stage framework, therefore, we need to consider the day-ahead scheduling cost in the first stage and dispatch or recourse cost in the second stage for the objective function. In particular, the first-stage cost includes start-up, shut-down, and no-load cost of MTs, the second-stage cost consists of fuel cost, degradation cost of ESS and TSS, and the electricity transaction cost with the main grid. This objective is assumed to be beneficial for the distribution system operator who can manage the microgrid by an energy management system. Mathematically, the objective function is represented as follows:

$$C^{\text{tot}} = \sum_t \sum_i (\text{SU}_i y_{it}^+ + \text{SD}_i y_{it}^- + c_i^{\text{NL}} y_{it}) + \max_{\mathbf{P} \in \mathcal{D}} E_{\mathbf{P}}[Q(\mathbf{y}, \mathbf{w})] \quad (24)$$

$$Q(\mathbf{y}, \mathbf{w}) = \sum_{t=1}^T \left\{ c^{\text{gas}} \left( \sum_{i=1}^{N^{MT}} F_{it}^{\text{MT}} + \sum_{g=1}^{N^{\text{GF}}} F_{it}^{\text{GF}} \right) + \sum_j c_j^e (r_{jt}^+ \eta_j^+ + r_{jt}^- / \eta_j^-) + \sum_m c_m^q (r_{mt}^q \eta_m^q + r_{mt}^q / \eta_m^q) + (c_t^{\text{buy}} p_t^{\text{buy}} - c_t^{\text{sell}} p_t^{\text{sell}}) \right\} \quad (25)$$

where  $C^{\text{tot}}$  represents the total cost including the first-stage and second-stage cost, set  $\mathcal{D}$  is the ambiguity set for uncertain wind power  $\mathbf{w}$ ,  $Q(\cdot)$  is the second-stage operational cost, and  $\mathbf{y}$  represents the first-stage decision variables. In the second stage, the scheduling cost from different forms of energy sources can also be calculated, which helps analyse the various energy consumption in a multi-energy system including the consumption of MTs, storage system, and utility grid. The parameter values in the objective function will be introduced in case studies. In addition, a simple linear degradation cost is used here for storage systems to avoid frequent charging and discharging, which would affect the storage lifetime [14]. Although degradation is a highly complex and non-linear phenomenon in practice, it is not the main focus of this work and a linear approximation cost is adopted here. Note that deterministic prices are used here since we mainly focus on the uncertainty of renewable generation in this work, i.e. the robust formulation aims for uncertain renewable generation, and other factors may be assumed to be uncertain for future research. Specifically, some uncertainties from the demand side including load demand uncertainty and outage can be considered in the future.

#### 2.4 Multi-period formulation

For notational conciseness, the general two-stage CCHP-based microgrid model introduced above can be written in a compact matrix formulation as follows:

$$\min_{\mathbf{y} \in \mathcal{Y}} \mathbf{a}^T \mathbf{y} + \max_{\mathbf{P} \in \mathcal{D}} E_{\mathbf{P}}[Q(\mathbf{y}, \mathbf{w})] \quad (26a)$$

$$Q(\mathbf{y}, \mathbf{w}) = \min_{\mathbf{x}} \{ \mathbf{b}^T \mathbf{x} : \mathbf{T}\mathbf{y} + \mathbf{W}\mathbf{x} \geq \mathbf{h} - \mathbf{H}\mathbf{w} \} \quad (26b)$$

where set  $\mathcal{Y}$  represents the first-stage constraints including constraints (3)–(6), the matrix inequality expression in (26b) consists of the second-stage constraints (1)–(2) and (7)–(23), and the second-stage decision variables are collected in  $\mathbf{x}$ . The coefficient matrices  $\mathbf{T}$ ,  $\mathbf{W}$ ,  $\mathbf{H}$  and vector  $\mathbf{h}$  can be elicited from these constraints and they are sparse.

As discussed above, in a common two-stage model, UC decision is usually considered in the first stage and recourse decision is studied in the second stage. However, there is an unrealistic assumption that non-anticipativity is not considered in the second stage. In other words, it is assumed that the second-stage dispatch decisions are optimised simultaneously with the disclosure of all uncertainty realisations in the beginning [33]. However, the uncertain wind power is revealed sequentially in practice and the dispatch decisions can only be made according to the uncertainty realisations up to current period, i.e. the dispatch decision at time  $t$  is dependent on the wind power realisations from time 1 to  $t$ , which can be expressed as  $\mathbf{w}_{[t]}$ . Note that a multi-period is used here to represent the multiple time periods in this work, which differentiates it from the name stage. Accordingly, the two-stage multi-period problem enforcing non-anticipativity can be formulated as follows:

$$\min_{\mathbf{y} \in \mathcal{Y}, \mathbf{x}(\cdot)} \mathbf{a}^T \mathbf{y} + \max_{\mathbf{P} \in \mathcal{D}} E_{\mathbf{P}}[\mathbf{b}^T \mathbf{x}(\mathbf{w}_{[t]})] \quad (27a)$$

$$\text{s. t. } \mathbf{T}\mathbf{y} + \mathbf{W}\mathbf{x}(\mathbf{w}_{[t]}) \geq \mathbf{h} - \mathbf{H}\mathbf{w} \quad (27b)$$

where  $\mathbf{x}(\mathbf{w}_{[t]})$  represents a function of  $\mathbf{w}_{[t]}$ , and this implies that the recourse decision only has a relationship with the uncertainty realisations up to time  $t$  instead of the whole set including future realisations. The consideration of non-anticipativity is the main difference between the proposed model and the common two-stage models. Generally, the distributionally robust multi-period problem is complex and intractable, and the solution method will be introduced in the next section.

### 3 Solution methodology

In this section, the ambiguity set for wind power is first designed to describe its possible probability distribution, then the linear decision rule approach is introduced to approximate the multi-period problem, and the intractable distributionally robust multi-period problem is finally reformulated as a tractable problem.

#### 3.1 Ambiguity set for wind power

In the DRO method, an ambiguity set is used to capture all possible probability distributions of random variables sharing common statistical characteristics such as moment information. In this work, we also design a new ambiguity set based on moment information of wind power [34]. More specifically, by defining  $\mathbf{w}_{[t]} = (\mathbf{w}_1, \dots, \mathbf{w}_t)$  and  $\mathbf{w}_t = (w_{nt})$ , the studied ambiguity set is given below

$$\mathcal{D} = \left\{ \mathbf{P} \in \mathcal{P}_0(\mathbb{R}^{N^w T}) \left| \begin{array}{l} \mathbb{P}(\mathbf{w} \in \mathcal{W}) = 1, \\ E_{\mathbf{P}}(\mathbf{w}) = \boldsymbol{\mu}, \\ E_{\mathbf{P}}((w_{nt} - \mu_{nt})^2) \leq \sigma_{nt}, \forall n, t, \\ E_{\mathbf{P}}\left[\left(\sum_{l=k}^t \mathbf{1}^T (\mathbf{w}_l - \boldsymbol{\mu}_l)\right)^2\right] \leq \gamma_{kt}, \\ \forall k \leq t, t \in [T] \end{array} \right. \right\} \quad (28)$$

where  $\mathcal{P}_0(\cdot)$  is the set of all distributions,  $\mathcal{W}$  is the support set defined as  $\mathcal{W} = [\underline{\mathbf{w}}, \bar{\mathbf{w}}]$ ,  $\boldsymbol{\mu}$  is the estimated mean vector of wind power,  $\sigma_{nt}$  and  $\gamma_{kt}$  are parameters related to variance, which can be

used to adjust the conservatism. The parameters in this set can be estimated from historical wind power data, i.e. the set can be constructed in a data-driven manner. Specifically, we can collect  $N$  data samples  $\{\mathbf{w}^i\}_{i=1}^N$  first with  $\mathbf{w}^i = [w_1, w_2, \dots, w_T]^\top$ , then  $\underline{\mathbf{w}}$  and  $\overline{\mathbf{w}}$  can be set to be the minimum and maximum values of these samples, respectively.  $\boldsymbol{\mu}$  can be estimated from the sample mean  $\sum_{i=1}^N \mathbf{w}^i / N$ .  $\sigma_{nt}$  and  $\gamma_{kt}$  can be obtained from the covariance matrix  $\Phi = \sum_{i=1}^N (\mathbf{w}^i - \boldsymbol{\mu})(\mathbf{w}^i - \boldsymbol{\mu})^\top / N$ . In other words,  $\sigma_{nt}$  corresponds to the diagonal element, and  $\gamma_{kt}$  is the sum of specific elements in matrix  $\Phi$ , i.e.  $\gamma_{kt} = \mathbf{f}_{kt}^\top \Phi \mathbf{f}_{kt}$ , where  $\mathbf{f}_{kt}$  is a vector with one in the  $j$ th position if  $j$  falls in the time window  $[k, t]$  and zero in the other positions. Note that the support set here is significant which can avoid some extreme distributions and negative wind power values. In addition, we only consider the uncertainty of generation side in this work, and the uncertainty from demand side such as load can be studied in the future.

There are two main features in the ambiguity set introduced above. First, the partial cross-moment information is included, which helps capture both the temporal correlation and spatial correlation of wind power [35]. Second, this set is a second-order conic representable set and the corresponding DRO problem can be transformed into a second-order conic programme, which can be solved by many off-the-shelf solvers. To obtain a tractable DRO problem with the set (28), the following lifted ambiguity set is proposed [34] by introducing auxiliary variables, which keep the optimal solution equivalent:

$$\overline{\mathcal{D}} = \left\{ \begin{array}{l} \mathbb{P} \in \mathcal{P}_0(\mathbb{R}^{N^*T} \times \mathbb{R}^{N^*T} \times \mathbb{R}^{T(T+1)/2}) \\ \mathbb{P}((\mathbf{w}, \mathbf{u}, \mathbf{v}) \in \overline{\mathcal{W}}) = 1, \\ E_{\mathbb{P}}(\mathbf{w}) = \boldsymbol{\mu}, \\ E_{\mathbb{P}}(u_{nt}) \leq \sigma_{nt}, \forall n, t, \\ E_{\mathbb{P}}(v_{kt}) \leq \gamma_{kt}, \forall k \leq t, t \in [T] \end{array} \right\} \quad (29)$$

where  $\mathbf{u}$  and  $\mathbf{v}$  are auxiliary variables, and  $\overline{\mathcal{W}}$  is the lifted support set defined as below

$$\overline{\mathcal{W}} = \left\{ (\mathbf{w}, \mathbf{u}, \mathbf{v}) \left| \begin{array}{l} \underline{\mathbf{w}} \leq \mathbf{w} \leq \overline{\mathbf{w}}, \\ (w_{nt} - \mu_{nt})^2 \leq u_{nt}, \forall n, t, \\ [\sum_{l=k}^t \mathbf{1}'(\mathbf{w}_l - \boldsymbol{\mu}_l)]^2 \leq v_{kt}, \\ \forall k \leq t, t \in [T] \end{array} \right. \right\}. \quad (30)$$

With the auxiliary variables in (29), the non-linear constraints in the original ambiguity set are eliminated, i.e. the fourth and fifth row in  $\overline{\mathcal{D}}$  are linear constraints, and this helps reformulate the second-stage problem with dual theory and makes the problem tractable as introduced later in the problem reformulation.

It is equivalent to deal with the DRO problem with the lifted ambiguity set since the original set  $\mathcal{D}$  is equivalent to the set of marginal distributions of  $\mathbf{w}$  under all  $\mathbb{P} \in \overline{\mathcal{D}}$ . In addition, we can further design tighter lifted support set  $\tilde{\mathcal{W}}$  by incorporating the upper bounds of  $\mathbf{u}$  and  $\mathbf{v}$ , which can significantly improve the performance of the optimal solution, and the improvement is verified in case studies. Set  $\tilde{\mathcal{W}}$  is expressed as follows:

$$\tilde{\mathcal{W}} = \{\overline{\mathcal{W}}, u_{nt} \leq \bar{u}_{nt}, v_{kt} \leq \bar{v}_{kt}, \forall n, t, k \leq t\} \quad (31)$$

where the upper bounds can be obtained as  $\bar{u}_{nt} = \max\{(w_{nt} - \mu_{nt})^2, (\bar{w}_{nt} - \mu_{nt})^2\}$  and  $\bar{v}_{kt} = \max\{(\sum_{l=k}^t \mathbf{1}'(\mathbf{w}_l - \boldsymbol{\mu}_l))^2, (\sum_{l=k}^t \mathbf{1}'(\bar{\mathbf{w}}_l - \boldsymbol{\mu}_l))^2\}$ .

### 3.2 Linear decision rule

The multi-period problem (27) is computationally challenging since the recourse variable  $\mathbf{x}$  is a function of all past uncertainty realisations. In addition, the explicit expression of the recourse

policy and worst-case expectation are generally intractable to acquire. One effective approach to solve this multi-period problem is the LDR method, which is also known as affine decision rule [20, 36]. The LDR method enforces the recourse variable to be linearly dependent on some random variables to overcome the intractability. Actually, the LDR method depending on all past uncertainty realisations prior to time  $t$  still makes the problem very computationally difficult, thus we adopt a simplified LDR method in this work, which has been demonstrated to be a sufficiently good approximation method [24]. Although this method is an approximation method, it is a good compromise to solve the intractable problem since the true relationship between the recourse variable and uncertain parameters is unknown. Note that other decision rules may also be studied to explore the true relationship. In the simplified LDR method, the recourse variable is assumed to be a linear function of the uncertain parameters at the current time period. Particularly, the LDR method for a single recourse variable can be expressed as follows:

$$x_i(\mathbf{w}_{[t]}, \mathbf{u}_{[t]}) = x_i^0 + \sum_n x_{nt}^w w_{nt} + \sum_n x_{nt}^u u_{nt} \quad (32)$$

where  $x_i^0$  is a constant,  $x_{nt}^w$  and  $x_{nt}^u$  are related linear coefficients, which will be considered as decision variables in the new problem. In addition, the auxiliary variable  $u_{nt}$  is also included in this LDR method since this enhanced LDR method can improve the results as shown in [34]. Since the variables  $u_{nt}$  and  $v_{kt}$  are both related with the second-order moment information,  $v_{kt}$  is neglected here to reduce the number of decision variables.

Based on (32), we can write the LDR method for all recourse variables, i.e. the recourse variables of the whole horizon in a matrix form as follows:

$$\mathbf{x}(\mathbf{w}, \mathbf{u}) = \mathbf{x}^0 + \mathbf{X}^w \mathbf{w} + \mathbf{X}^u \mathbf{u} \quad (33)$$

where  $\mathbf{x}^0$  denotes the constant vector,  $\mathbf{X}^w$  and  $\mathbf{X}^u$  are coefficients matrices,  $\mathbf{w} = (w_1^\top, w_2^\top, \dots, w_T^\top)^\top$  is the vector of wind power. With the LDR method, the non-anticipativity is automatically included and a tractable problem can be obtained for the complex multi-period problem.

### 3.3 Problem reformulation

To solve the proposed two-stage multi-period distributionally robust problem for CCHP-based microgrid system, we need to reformulate it into a tractable problem. First, the second-stage worst-case expectation  $\max_{\mathbb{P} \in \overline{\mathcal{D}}} E_{\mathbb{P}}[\mathbf{b}^\top \mathbf{x}]$  in the two-stage framework needs to be addressed to reduce the computational burden [37]. The worst-case expectation can be written in an integral form as below

$$\max_{\mathbb{P} \in \overline{\mathcal{D}}} \int_{\overline{\mathcal{W}}} (\mathbf{b}^\top \mathbf{x}) dP(\mathbf{w}, \mathbf{u}, \mathbf{v}) \quad (34a)$$

$$\text{s.t.} \int_{\overline{\mathcal{W}}} dP(\mathbf{w}, \mathbf{u}, \mathbf{v}) = 1: (\lambda) \quad (34b)$$

$$\int_{\overline{\mathcal{W}}} \mathbf{w} dP(\mathbf{w}, \mathbf{u}, \mathbf{v}) = \boldsymbol{\mu}: (\boldsymbol{\eta}) \quad (34c)$$

$$\int_{\overline{\mathcal{W}}} u_{nt} dP(\mathbf{w}, \mathbf{u}, \mathbf{v}) \leq \sigma_{nt}, \forall n, t: (\beta_{nt}) \quad (34d)$$

$$\int_{\overline{\mathcal{W}}} v_{kt} dP(\mathbf{w}, \mathbf{u}, \mathbf{v}) \leq \gamma_{kt}, \forall k \leq t: (\alpha_{kt}) \quad (34e)$$

where the symbols in the parenthesis are related dual variables that are used later. According to the strong duality, the equivalent dual problem of (34) is given as follows [34, 37]:

$$\min_{\lambda, \eta, \beta \geq 0, \alpha \geq 0} \lambda + \eta^T \mu + \beta^T \sigma + \alpha^T \gamma \quad (35a)$$

$$\text{s. t. } \lambda + \eta^T w + \beta^T u + \alpha^T v \geq b^T x, \forall (w, u, v) \in \overline{\mathcal{W}} \quad (35b)$$

where  $\beta$  and  $\alpha$  are corresponding dual vectors composed of  $\beta_{nt}$  and  $\alpha_{nt}$ , respectively.

By combining the first-stage problem with (35) and considering the LDR method in (33), we can get the following equivalent formulation of the two-stage multi-period problem (27):

$$\begin{aligned} \min_{y \in \mathcal{Y}} a^T y + \min_{\lambda, \eta, \beta \geq 0, \alpha \geq 0} \lambda + \eta^T \mu + \beta^T \sigma + \alpha^T \gamma \\ \text{s. t. } \lambda + \eta^T w + \beta^T u + \alpha^T v \geq \\ b^T (x^0 + X^w w + X^u u), \forall (w, u, v) \in \overline{\mathcal{W}} \end{aligned} \quad (36a)$$

$$Ty + W(x^0 + X^w w + X^u u) \geq h - Hw. \quad (36b)$$

Constraints (36a) and (36b) can be further recast equivalently as follows:

$$\lambda - b^T x^0 \geq \max_{(w, u, v) \in \overline{\mathcal{W}}} [(b^T X^w)^T - \eta]^T w + [(b^T X^u)^T - \beta]^T u - \alpha^T v \quad (37a)$$

$$Ty - h + Wx^0 \geq \max_{(w, u, v) \in \overline{\mathcal{W}}} (-WX^w - H)w - WX^u u. \quad (37b)$$

Note that the above two constraints are actually robust constraints with the support set  $\overline{\mathcal{W}}$  and they have the same structure. To eliminate the max operator on the right-hand side, the maximisation problem can be transformed into a minimisation problem based on dual theory, and the minimisation problem is equivalent to the existence of a feasible solution where the min operator can be neglected. Take constraint (37a) as an example, and we can get the dual problem of the right maximisation based on conic duality [33, 38] as follows:

$$\begin{aligned} \min_{\psi} \bar{w}^T \bar{\delta} - \underline{w}^T \bar{\delta} - \mu^T \bar{\theta} - \frac{1}{2} \mathbf{1}^T \bar{\theta} + \frac{1}{2} \mathbf{1}^T \hat{\theta} \\ - \sum_t \sum_{k \in [1:t]} \sum_{l=k}^t \mathbf{1}^T \mu_l \bar{\rho}_{kl} - \frac{1}{2} \mathbf{1}^T \bar{\rho} + \frac{1}{2} \mathbf{1}^T \hat{\rho} \end{aligned} \quad (38a)$$

$$\bar{\delta}_{nt} - \bar{\delta}_{nt} + \bar{\theta}_{nt} + \sum_{k=1}^t \sum_{l=t}^T \bar{\rho}_{kl} = e_{nt}^T (\eta - (b^T X^w)^T), \quad \forall t, n \quad (38b)$$

$$(\bar{\theta}_{nt} + \hat{\theta}_{nt})/2 = e_{nt}^T [\beta - (b^T X^u)^T], \quad \forall t, n \quad (38c)$$

$$(\bar{\rho}_{kt} + \hat{\rho}_{kt})/2 = \alpha_{kt}, \quad \forall t, k \leq t \quad (38d)$$

$$\sqrt{(\bar{\theta}_{nt}^2 + \hat{\theta}_{nt}^2)} \leq \hat{\theta}_{nt}, \quad \forall t, n \quad (38e)$$

$$\sqrt{(\bar{\rho}_{kt}^2 + \hat{\rho}_{kt}^2)} \leq \hat{\rho}_{kt}, \quad \forall t, k \leq t \quad (38f)$$

where  $\psi = \{\bar{\delta}, \underline{\delta}, \bar{\theta}, \hat{\theta}, \bar{\rho}, \hat{\rho}, \hat{\rho}\}$  are dual variables corresponding to the constraints in  $\overline{\mathcal{W}}$ ,  $\mathbf{1}$  is a vector with all 1 elements, and  $e_{nt}$  is a zero vector except that the  $(2(t-1) + n)$ th element is 1. Thus, constraint (37a) is recast as follows:

$$\begin{aligned} \lambda - b^T x^0 \geq \bar{w}^T \bar{\delta} - \underline{w}^T \bar{\delta} - \mu^T \bar{\theta} - \frac{1}{2} \mathbf{1}^T \bar{\theta} + \frac{1}{2} \mathbf{1}^T \hat{\theta} \\ - \sum_t \sum_{k \in [1:t]} \sum_{l=k}^t \mathbf{1}^T \mu_l \bar{\rho}_{kl} - \frac{1}{2} \mathbf{1}^T \bar{\rho} + \frac{1}{2} \mathbf{1}^T \hat{\rho} \end{aligned} \quad (39a)$$

$$(38b)-(38f). \quad (39b)$$

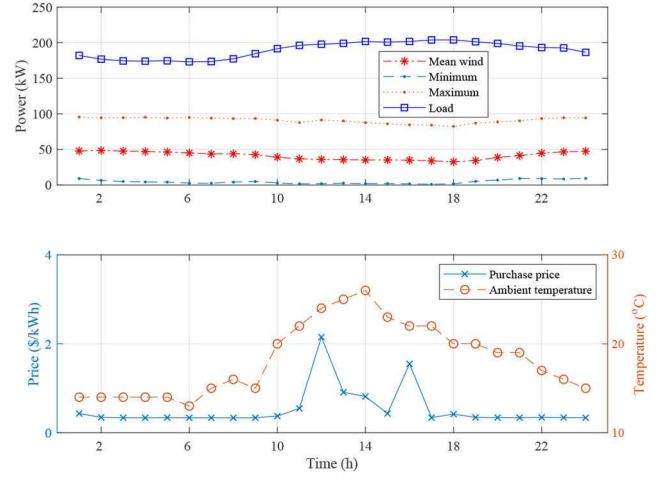


Fig. 3 Data profiles

Since constraint (37b) has the same structure with (37a), a similar approach can be applied to deal with (37b) by introducing new dual variables and replacing the right-hand side of the above dual constraints with the elements of the coefficient matrices of  $(w, u, v)$  in (37b), and the detailed formulation is omitted here. Therefore, constraints (37a) and (37b) are transformed into a finite number of linear and second-order conic constraints, and the original two-stage multi-period problem is finally reformulated as a tractable mixed-integer second-order conic programme (MISOCP) which is actually a single minimisation problem and can be solved by some off-the-shelf solvers.

## 4 Case studies

In this section, case studies are conducted to validate the performance of the proposed approach. First, related parameters are set and historical wind power data are collected to construct the ambiguity set. Then the simulation results and comparison with other methods are presented. All the experiments are implemented in the Matlab environment solved by the MOSEK solver [39] on a personal computer (Intel Core i7-6700 CPU 3.4 GHz and 8 GB RAM).

### 4.1 Data and parameter settings

In this work, a CCHP-based microgrid composed of three MTs, a gas furnace, two wind farms, one energy storage, and a thermal storage system, and electric and thermal loads, which are all in a single bus system is considered. The main focus of this work is on small-scale systems, a larger system considering the network constraints in the second stage problem may be studied in the future. The optimisation horizon is  $T = 24$  h with a scale of 1 h. The studied CCHP-based microgrid is a virtual system with typical components and settings, and the hourly wind power data of the last month in 2018 from [40] are used, which are the latest in the dataset. Then, we can estimate the mean, upper, and lower bounds used in the ambiguity set as shown in Fig. 3, which are properly scaled. It is assumed that two wind farms have the same power profile for simplicity and the wind generation capacity is 100 kW. In addition, the other parameters in the ambiguity set can also be estimated from the data with the covariance matrix. The scaled electric load and purchase price are collected from AESO [41], the forecast ambient temperature of Edmonton on 16 July is used here, which is related to the thermal load, and they are all shown in Fig. 3. In addition, the price of selling electricity to the main grid is assumed to be 0.8 of the purchase price.

The main parameters of MTs are given in Table 1, which are collected from relevant references [3, 33]. In addition, the start-up (shut-down) costs of three MTs are 3, 3, and 1.5, respectively, and the no-load operation costs are 3, 6, and 1, respectively. The rest parameter values about the gas furnace, storage systems, and other constraints used in this work are listed in Table 2, and these parameter values are common in related reference [13, 14].

**Table 1** Parameters of MTs

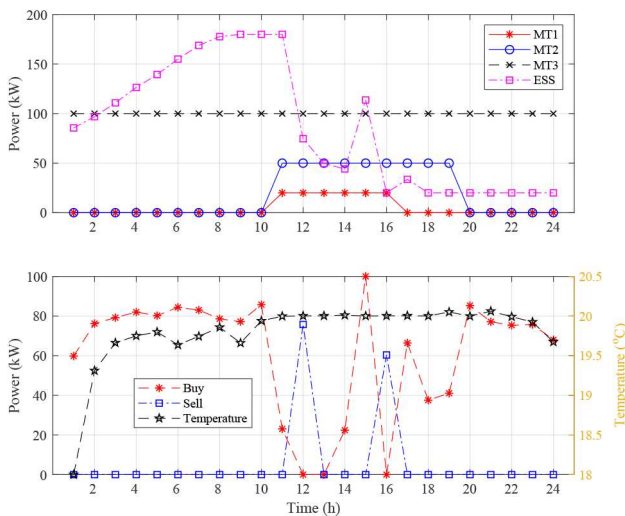
Unit	$\underline{p}_i$	$\bar{p}_i$	$DT_i$	$UT_i$	$R_i^{up}/R_i^{dn}$	$\eta_i^{MT}$	$\eta_{i,loss}^{MT}$
MT1	5	20	1	1	10	0.295	0.115
MT2	5	50	2	2	25	0.285	0.15
MT3	50	100	2	3	50	0.3	0.1

**Table 2** Main parameter values

Parameters	Value	Parameters	Value
$\eta_j^{e+}/\eta_j^{e-}$	0.95	$E_{m0}^q$	90 kWh
$\eta_m^{q+}/\eta_m^{q-}$	0.9	$\underline{E}_m^q/\bar{E}_m^q$	20/180 kWh
$\eta_s^{GF}$	0.93	$\underline{h}_g^{GF}/\bar{h}_g^{GF}$	0/80 kW
$\theta_t^{in}/\theta_t^{in}$	18/22°C	$\bar{p}^{AC}/\bar{p}^{HC}$	200 kW
$c^{air}$	1.85 kWh/m <sup>3</sup> °C	$H^G$	9.78 kWh/m <sup>3</sup>
$c^{gas}$	0.5 \$/m <sup>3</sup>	$\underline{r}_j^{e+}/\bar{r}_j^{e+}$	0/100 kW
$c_j^e/c_m^q$	0.0035 \$/kWh	$\underline{r}_j^{e-}/\bar{r}_j^{e-}$	0/100 kW
COP <sup>C</sup> /COP <sup>H</sup>	0.83/0.8	$\underline{r}_m^{q+}/\bar{r}_m^{q+}$	0/100 kW
$E_{j0}^e$	90 kWh	$\underline{r}_m^{q-}/\bar{r}_m^{q-}$	0/100 kW
$\underline{E}_j/\bar{E}_j$	20/180 kWh	$R^{tr}$	1.3 °C/kW

**Table 3** UC results of MTs

Hour	1	2	3	4	5	6	7	8	9	10	11	12	13	14	15	16	17	18	19	20	21	22	23	24
MT1	0	0	0	0	0	0	0	0	0	0	1	1	1	1	1	1	0	0	0	0	0	0	0	0
MT2	0	0	0	0	0	0	0	0	0	0	1	1	1	1	1	1	1	1	1	0	0	0	0	0
MT3	1	1	1	1	1	1	1	1	1	1	1	1	1	1	1	1	1	1	1	1	1	1	1	1

**Fig. 4** Output of recourse variables with LDR

#### 4.2 Simulation results

With the data and parameter settings introduced above, we can solve the two-stage multi-period CCHP-based microgrid energy management problem. First, the UC decisions of three MTs can be obtained, and the results are presented in Table 3. From this table, it can be seen that MT3 is always on to supply power since it has the lowest generation cost, while MT1 and MT2 are started up at time period 11 when the load increases. Therefore, the original intractable problem is successfully solved by the proposed technique, which also shows its effectiveness. The total cost for this case is \$115.13, including the first-stage UC cost \$108, and the second-stage operational cost \$7.13, and the solution time is about 38 min. This solution time is acceptable since hourly dispatch is usually considered in a UC problem as is done in this work.

To further verify the performance of the LDR method, the second-stage recourse variables for a realised wind power data are

investigated. In other words, the first-stage UC decisions are fixed, and the second-stage dispatch problem is studied. More specifically, the lower bounds of wind power data are used, and the output of MTs and the ESS storage level, the electricity transaction with the main grid, and indoor temperature settings are illustrated in Fig. 4. Note that since there are not so many thermal loads, in this case, the output of the gas furnace is close to zero, and the TSS is almost not used, hence, their output is not shown here. From Fig. 4, we can see that three MTs approximately generate the maximum output as a result of the low wind power. The ESS charges continually at first and starts to discharge after time period 11 when the load demand is high. For electricity transactions, it can be seen that the microgrid buys electricity from the main grid with low purchase prices most of the time and it sells electricity at time periods 12 and 16 when the selling electricity prices are very high. This shows the effectiveness of the policy, which helps maximise the profit of the microgrid system. In addition, the indoor temperature settings are also within the predefined comfortable range. In this case, the scheduling cost from different energy sources can also be obtained. For example, the dispatch costs of MT1, MT2, and MT3 are \$20.8, \$80.72, and \$153.37, respectively.

In addition to the temperature-dependent thermal loads, other thermal or heat loads can also be considered in the system, and this can be used to check the role of TSS in the system. In other words, a new parameter  $p_i^{\text{heat\_load}}$  representing the thermal loads can be added to the right side of the thermal load balance equation (16). In this case study, the thermal loads are assumed to be deterministic, which are half of the electric loads as shown in Fig. 3. With the same solution method, we can solve the problem, and the total cost objective is \$160.23 with the UC cost \$192 and the operational cost (profit) \$-31.77. Similarly, the realised lower bounds of wind power are used, and we can obtain the second-stage recourse variables with the LDR method, which are illustrated in Fig. 5. As can be seen from this figure, the MTs will run for a longer time (e.g. MT2) with the deployment of more thermal loads, which also results in the decrease of the electricity purchase from the main grid. For the storage systems, the state of ESS has a similar variation trend since the electric load stays unchanged, while the

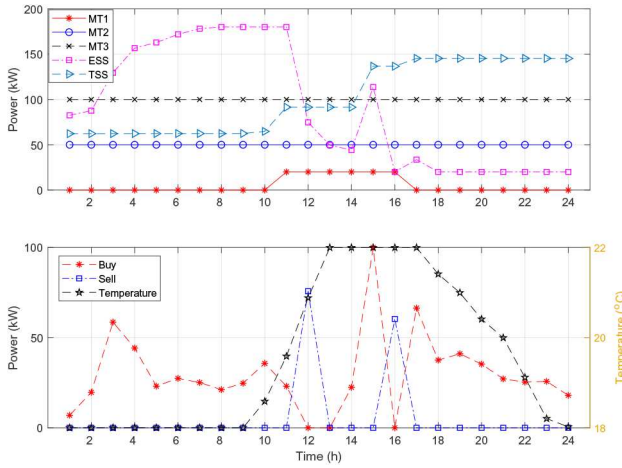


Fig. 5 Output of recourse variables with more thermal loads

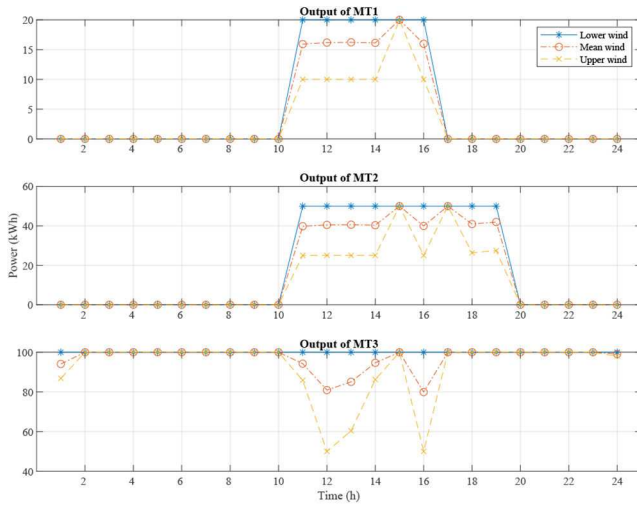


Fig. 6 Output variation of MTs with different wind power scenarios

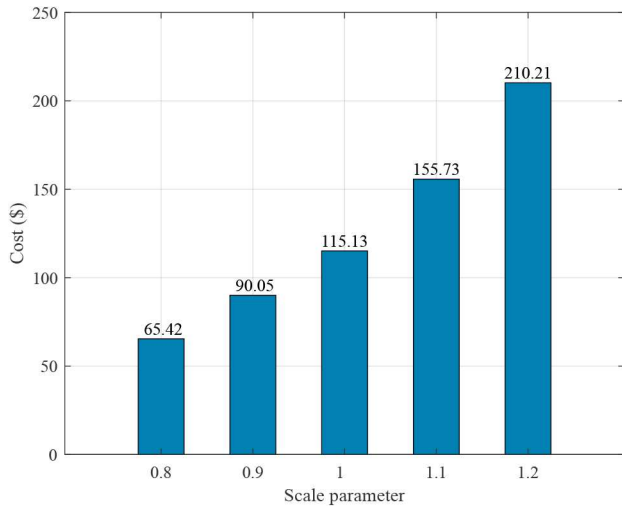


Fig. 7 Influence of different forecast intervals

Table 4 Comparison results

Method	DRO	DRO2	RO	Deterministic
total cost, \$	115.13	78.55	628.07	-74.20
UC cost, \$	108	147	240	126
operational cost, \$	7.13	-68.45	388.07	-200.20
reliability, %	100	100	100	64.46
penalty cost, \$	0	0	0	2109.62

TSS first discharges from the initial level and charges in later time to cope with the system state change caused by the increased thermal loads. Similarly, the microgrid system also sells electricity to the main grid at time periods 12 and 16 to maximise the profit when the selling prices are high. In other words, the electricity transaction is closely related to the variation of the electricity transaction prices. Also, the indoor temperature can be controlled within a comfortable range.

To further verify the performance of the proposed approach under different uncertainty scenarios, more case studies are investigated with different wind power scenarios. Specifically, three typical wind power scenarios, i.e. lower bound, mean, and upper bound of the wind power as shown in Fig. 3 are used to analyse the variation of dispatch decisions with the obtained LDR. For conciseness, only the output results of MTs are shown here as illustrated in Fig. 6. From this figure, it can be seen that the power outputs of three MTs all decrease properly with the increase of wind power. In addition, when the load demand is very high at some time periods, the MTs will have the maximum output under all scenarios. These results validate the effectiveness of the obtained solution in dealing with different uncertainty scenarios, and they also disclose the connection between dispatch using CCHP units and dispatch using renewable generation.

*Influence of forecast intervals:* In the proposed ambiguity set, a critical part is the forecast interval or support set of wind power, which is also closely related to the popular interval forecast topic. Therefore, to study the influence of interval size on the results, different forecast intervals are investigated in this work. In particular, a scale parameter  $\xi$  is introduced to adjust the upper bound of wind power, i.e.  $\xi \cdot \bar{w}$ . The value of  $\xi$  is set to be 0.8, 0.9, 1, 1.1, and 1.2, respectively, which helps change the interval size. Note that the adjustment of lower bound is not considered here since the lower bound is very close to zero. The cost results with different intervals are given in Fig. 7. As shown in this figure, the system cost increases with an increase of  $\xi$ . In other words, when the interval size becomes larger, the system cost is higher, i.e. more investment is required to cope with the increasing uncertainty. Hence, the accuracy of forecast intervals may be investigated to control the conservativeness of the solution when designing the ambiguity set.

#### 4.3 Comparison with other methods

In this subsection, the proposed CCHP-based microgrid energy management problem is further studied with the new support set  $\tilde{\mathcal{W}}$  to improve the solution, and the proposed approach is compared with other methods to validate its effectiveness. This method with a new support set can be considered as an improved DRO method compared with that with a general support set [34]. With set  $\tilde{\mathcal{W}}$ , which includes upper bounds of auxiliary variables, we can reformulate the problem similarly and the optimal cost achieved is \$78.55, which enhances the original objective. For comparison purposes, we study the problem with a robust optimisation (RO) approach and the deterministic method. RO is a popular method to deal with uncertainty, and it has been widely studied in microgrid energy management problems [13, 14]. In the RO method, the interval uncertainty set is used and the problem is solved with column and constraint generation (CCG) approach [14, 42]. For the deterministic method, fixed wind power realisations (e.g. mean values) are used and there is no uncertainty. The comparison results are summarised in Table 4 including the total cost, first-stage UC cost, and second-stage operational cost. In this table, DRO is the proposed method and DRO2 is the DRO method with new support set  $\tilde{\mathcal{W}}$ . From the total cost, we can find that the proposed DRO method is less conservative than the RO method, which schedules more units to guard against uncertainty. Moreover, the solution time of the RO method is about 52 min, which is longer. In the RO method, when we transform the second-stage problem or dualise the inner min problem, some bilinear terms will be generated which need to be addressed with a big-M method, and this introduces more variables and constraints, which results in longer computational time. In addition, the total cost (profits) of the deterministic method is better than the DRO method and the

computational time is about 21 s. However, there is no uncertainty information in the deterministic method and the wind power realisations are assumed to be known in the entire horizon. By contrast, the non-anticipativity of the multi-period problem is enforced in the proposed DRO method, which can deal with the uncertainty from renewable generation.

To better show the effectiveness of the proposed approach in cost reduction or robustness enhancement, an out-of-sample assessment is carried out with the obtained solution. Specifically, the obtained UC decision and second-stage policy are fixed, then the Monte Carlo simulation method is used to generate 1000 wind power scenarios and we calculate the power balance constraint to check the reliability of the solution. The wind power scenarios are generated within the intervals defined in the ambiguity set by uniform distribution, and they represent the realisation of uncertainty. If the power balance chance constraint is not satisfied, penalty cost can be introduced according to the deficient power. The penalty factor is 10 \$/kWh here [14]. Similarly, this out-of-sample assessment is also conducted with solutions obtained from the RO method and deterministic method. The reliability index and average penalty cost results are given in the last two rows of Table 4. From the table, it can be seen that both the proposed DRO method and the RO method can ensure the power balance for different uncertainty scenarios, while the deterministic method only has a reliability of 64.46%. As a result, a high average penalty cost is caused with the deterministic method and it is zero for the other methods. In addition, the proposed DRO method can reduce the conservativeness or UC cost of the RO method with the same robustness guarantee.

## 5 Conclusion

In this work, distributionally robust energy management for CCHP-based microgrids is investigated. Different from the previous literature, a two-stage multi-period model is proposed, which considers the non-anticipativity of the dispatch process. To capture the uncertainty of wind power, a second-order conic representable ambiguity set is designed based on moment information (e.g. mean and covariance), which can also describe the temporal and spatial correlation of random variable. With the LDR method, the complex multi-period problem is finally reformulated as a tractable MISOCP problem. In addition, a tight support set with upper bounds of auxiliary variables introduced in the lifted ambiguity set is investigated to further improve the solutions. The performance of the proposed approach is validated by case studies and comparison experiments based on real-world data. Particularly, the proposed DRO method can achieve a smaller cost (\$115.13) compared with the RO method (\$628.07), and it is less conservative than the RO method with the same reliability. In addition, although the cost of the deterministic method ( $-74.20$ ) is smaller than that of the DRO method, the reliability of the deterministic method is not good, which is only 64.46%, and this also results in a higher average penalty cost \$2109.62.

For future research, several topics may be studied to extend this work. For example, more uncertainty sources can be considered such as the uncertainty of electricity price and load demand. More microgrid components can be modelled and demand response can be integrated. In addition, the existing test system may be expanded to a larger distribution system by considering the complex network constraints.

## 6 Acknowledgments

This work was supported by the Natural Sciences and Engineering Research Council of Canada (NSERC). Z.S. was sponsored by the China Scholarship Council (CSC).

## 7 References

[1] Gu, W., Wang, Z., Wu, Z., *et al.*: 'An online optimal dispatch schedule for CCHP microgrids based on model predictive control', *IEEE Trans. Smart Grid*, 2017, **8**, (5), pp. 2332–2342

[2] Liu, M., Shi, Y., Fang, F.: 'Combined cooling, heating and power systems: a survey', *Renew. Sustain. Energy Rev.*, 2014, **35**, pp. 1–22

[3] Wang, J., Zhong, H., Xia, Q., *et al.*: 'Optimal joint-dispatch of energy and reserve for CCHP-based microgrids', *IET Gener. Transm. Distrib.*, 2017, **11**, (3), pp. 785–794

[4] Fang, F., Wang, Q.H., Shi, Y.: 'A novel optimal operational strategy for the CCHP system based on two operating modes', *IEEE Trans. Power Syst.*, 2012, **27**, (2), pp. 1032–1041

[5] Jiang, Y., Xu, J., Sun, Y., *et al.*: 'Coordinated operation of gas-electricity integrated distribution system with multi-CCHP and distributed renewable energy sources', *Appl. Energy*, 2018, **211**, pp. 237–248

[6] Li, G., Zhang, R., Jiang, T., *et al.*: 'Optimal dispatch strategy for integrated energy systems with CCHP and wind power', *Appl. Energy*, 2017, **192**, pp. 408–419

[7] Othman, A.M., El-Fergany, A.A.: 'Design of robust model predictive controllers for frequency and voltage loops of interconnected power systems including wind farm and energy storage system', *IET Gener. Transm. Distrib.*, 2018, **12**, (19), pp. 4276–4283

[8] Barik, A.K., Das, D.C.: 'Proficient load-frequency regulation of demand response supported bio-renewable cogeneration based hybrid microgrids with quasi-oppositional selfish-herd optimisation', *IET Gener. Transm. Distrib.*, 2019, **13**, (13), pp. 2889–2898

[9] Alipour, M., Mohammadi-Ivatloo, B., Zare, K.: 'Stochastic scheduling of renewable and CHP-based microgrids', *IEEE Trans. Ind. Inf.*, 2015, **11**, (5), pp. 1049–1058

[10] Bao, Z., Zhou, Q., Yang, Z., *et al.*: 'A multi time-scale and multi energy-type coordinated microgrid scheduling solution-part I: model and methodology', *IEEE Trans. Power Syst.*, 2015, **30**, (5), pp. 2257–2266

[11] Li, Z., Xu, Y.: 'Temporally-coordinated optimal operation of a multi-energy microgrid under diverse uncertainties', *Appl. Energy*, 2019, **240**, pp. 719–729

[12] Wang, Y., Tang, L., Yang, Y., *et al.*: 'A stochastic-robust coordinated optimization model for CCHP micro-grid considering multi-energy operation and power trading with electricity markets under uncertainties', *Energy*, 2020, **198**, p. 117273, <https://doi.org/10.1016/j.energy.2020.117273>

[13] Zhang, C., Xu, Y., Li, Z., *et al.*: 'Robustly coordinated operation of a multi-energy microgrid with flexible electric and thermal loads', *IEEE Trans. Smart Grid*, 2019, **10**, (3), pp. 2765–2775

[14] Guo, Y., Zhao, C.: 'Islanding-aware robust energy management for microgrids', *IEEE Trans. Smart Grid*, 2018, **9**, (2), pp. 1301–1309

[15] Aghaei, J., Agelidis, V.G., Charwand, M., *et al.*: 'Optimal robust unit commitment of CHP plants in electricity markets using information gap decision theory', *IEEE Trans. Smart Grid*, 2017, **8**, (5), pp. 2296–2304

[16] Delage, E., Ye, Y.: 'Distributionally robust optimization under moment uncertainty with application to data-driven problems', *Oper. Res.*, 2010, **58**, (3), pp. 595–612

[17] Wiesemann, W., Kuhn, D., Sim, M.: 'Distributionally robust convex optimization', *Oper. Res.*, 2014, **62**, (6), pp. 1358–1376

[18] Lu, X., Chan, K.W., Xia, S., *et al.*: 'Security-constrained multiperiod economic dispatch with renewable energy utilizing distributionally robust optimization', *IEEE Trans. Sustain. Energy*, 2019, **10**, (2), pp. 768–779

[19] Wei, W., Liu, F., Mei, S.: 'Distributionally robust co-optimization of energy and reserve dispatch', *IEEE Trans. Sustain. Energy*, 2016, **7**, (1), pp. 289–300

[20] Xiong, P., Jirutitijaroen, P., Singh, C.: 'A distributionally robust optimization model for unit commitment considering uncertain wind power generation', *IEEE Trans. Power Syst.*, 2017, **32**, (1), pp. 39–49

[21] Zhang, Y., Shen, S., Mathieu, J.L.: 'Distributionally robust chance-constrained optimal power flow with uncertain renewables and uncertain reserves provided by loads', *IEEE Trans. Power Syst.*, 2017, **32**, (2), pp. 1378–1388

[22] Shi, Z., Liang, H., Huang, S., *et al.*: 'Distributionally robust chance-constrained energy management for islanded microgrids', *IEEE Trans. Smart Grid*, 2019, **10**, (2), pp. 2234–2244

[23] Qiu, H., Gu, W., Xu, Y., *et al.*: 'Multi-time-scale rolling optimal dispatch for ac/dc hybrid microgrids with day-ahead distributionally robust scheduling', *IEEE Trans. Sustain. Energy*, 2019, **10**, (4), pp. 1653–1663

[24] Lorca, A., Sun, X.A.: 'Multistage robust unit commitment with dynamic uncertainty sets and energy storage', *IEEE Trans. Power Syst.*, 2017, **32**, (3), pp. 1678–1688

[25] Fatouros, P., Konstantelos, I., Papadaskalopoulos, D., *et al.*: 'Stochastic dual dynamic programming for operation of der aggregators under multi-dimensional uncertainty', *IEEE Trans. Sustain. Energy*, 2019, **10**, (1), pp. 459–469

[26] Shi, Z., Liang, H., Huang, S., *et al.*: 'Multistage robust energy management for microgrids considering uncertainty', *IET Gener. Transm. Distrib.*, 2019, **13**, (10), pp. 1906–1913

[27] Hjelmeland, M.N., Zou, J., Helseth, A., *et al.*: 'Nonconvex medium-term hydropower scheduling by stochastic dual dynamic integer programming', *IEEE Trans. Sustain. Energy*, 2018, **10**, (1), pp. 481–490

[28] Parisio, A., Wiezorek, C., Kyntäjä, T., *et al.*: 'An MPC-based energy management system for multiple residential microgrids'. Proc. IEEE Int. Conf. on Automation Science and Engineering (CASE), Gothenburg, Sweden, August 2015, pp. 7–14

[29] Evangelopoulos, V.A., Avramidis, I.I., Georgilakis, P.S.: 'Flexibility services management under uncertainties for power distribution systems: stochastic scheduling and predictive real-time dispatch', *IEEE Access*, 2020, **8**, pp. 38855–38871

[30] Zhang, Y., Meng, F., Wang, R., *et al.*: 'A stochastic MPC based approach to integrated energy management in microgrids', *Sustain. Cities Soc.*, 2018, **41**, pp. 349–362

[31] Li, Z., Guo, Q., Sun, H., *et al.*: 'Sufficient conditions for exact relaxation of complementarity constraints for storage-concerned economic dispatch', *IEEE Trans. Power Syst.*, 2016, **31**, (2), pp. 1653–1654

- [32] Chen, X., Xia, Q., Kang, C., *et al.*: 'A rural heat load direct control model for wind power integration in China'. IEEE Power and Energy Society General Meeting, San Diego, USA, July 2012, pp. 1–6
- [33] Babaei, S., Zhao, C., Fan, L.: 'A data-driven model of virtual power plants in day-ahead unit commitment', *IEEE Trans. Power Syst.*, 2019, **34**, (6), pp. 5125–5135
- [34] Bertsimas, D., Sim, M., Zhang, M.: 'Adaptive distributionally robust optimization', *Manage. Sci.*, 2018, **65**, (2), pp. 604–618
- [35] He, L., Hu, Z., Zhang, M.: 'Robust repositioning for vehicle sharing', *Manuf. Serv. Oper. Manage.*, 2020, **22**, (2), pp. 241–256
- [36] Shang, C., You, F.: 'Distributionally robust optimization for planning and scheduling under uncertainty', *Comput. Chem. Eng.*, 2018, **110**, pp. 53–68
- [37] He, C., Zhang, X., Liu, T., *et al.*: 'Distributionally robust scheduling of integrated gas-electricity systems with demand response', *IEEE Trans. Power Syst.*, 2019, **34**, (5), pp. 3791–3803
- [38] Lobo, M.S., Vandenberghe, L., Boyd, S., *et al.*: 'Applications of second-order cone programming', *Linear Algebra Appl.*, 1998, **284**, (1–3), pp. 193–228
- [39] MOSEK. Available from <https://www.mosek.com/>
- [40] Hourly aggregated wind power data. Available at <http://www.ercot.com/gridinfo/generation/>, accessed 15 July 2019
- [41] AESO. Available at <https://www.aeso.ca/market/market-and-system-reporting/>, accessed 15 July 2019
- [42] Zeng, B., Zhao, L.: 'Solving two-stage robust optimization problems using a column-and-constraint generation method', *Oper. Res. Lett.*, 2013, **41**, (5), pp. 457–461